Acta Crystallographica Section C
Crystal Structure Communications
ISSN 0108-2701

Bis[tris(2,2′-bipyridine-κ^2N,N')-ruthenium(II)] hexacyanoferrate(III) chloride octahydrate

Ken Sakai,[a]* Yuichi Uchida,[a] Takashi Kajiwara[b] and Tasuku Ito[b]

[a]Department of Applied Chemistry, Faculty of Science, Tokyo University of Science, Kagurazaka 1-3, Shinjuku-ku, Tokyo 162-8601, Japan, and [b]Department of Chemistry, Graduate School of Science, Tohoku University, Sendai 980-8578, Japan
Correspondence e-mail: ksakai@rs.kagu.tus.ac.jp

Received 20 November 2003
Accepted 15 December 2003
Online 17 January 2004

In the title compound, $[\mathrm{Ru^{II}(C_{10}H_8N_2)_3}]_2[\mathrm{Fe^{III}(CN)_6}]\mathrm{Cl}\cdot 8\mathrm{H_2O}$, the $[\mathrm{Ru(bpy)_3}]^{2+}$ (bpy is 2,2′-bipyridine) cations and water molecules afford intriguing microporous honeycomb layers, while the $[\mathrm{Fe(CN)_6}]^{3-}$ anions and the remainder of the water molecules form anionic sheets based on extensive hydrogen-bonding networks. The cationic and anionic layers alternate along the *c* axis. The Fe atom in $[\mathrm{Fe(CN)_6}]^{3-}$ lies on an inversion centre and the axial cyano ligands are hydrogen bonded to the water molecules encapsulated within the micropores [N···O = 2.788 (5) Å], giving an unusual interpenetration between the cationic and anionic layers. On the other hand, the in-plane cyano ligands are relatively weakly hydrogen bonded to the water molecules [N···O = 2.855 (7) and 2.881 (8) Å] within the anionic sheets.

Comment

We previously discovered that amidate-bridged *cis*-diammineplatinum(II) dimers, $[\mathrm{Pt_2(NH_3)_4}(\mu\text{-amidato})_2]^{2+}$ (amidate is acetamidate, α-pyrrolidinonate, α-pyridonate *etc.*), serve as efficient homogeneous catalysts in the photoreduction of water into molecular hydrogen (Sakai & Matsumoto, 1990; Sakai *et al.*, 1993). Since then, efforts have also been made to develop 'photomolecular devices evolving molecular hydrogen from water'. With this aim, a well known photosystem consisting of $[\mathrm{Ru(bpy)_3}]^{2+}$ (bpy is 2,2′-bipyridine) and methylviologen (usually *N*,*N*′-dimethyl-4,4′-bipyridinium dichloride; Borgarello *et al.*, 1981) has been employed to evaluate the catalytic activity of various platinum complexes. In this context, we started five years ago to explore the chemistry of double salts containing $[\mathrm{Ru(bpy)_3}]^{2+}$ and the various platinum complexes. Our aim has been to develop water-insoluble crystals involving both photosensitizers and $\mathrm{H_2}$-evolving catalysts. Visible-light-induced splitting of water into $\mathrm{H_2}$ and $\mathrm{O_2}$ might be promoted under dispersion of such hybrid crystals in water. As part of these studies, we report here the crystal structure of the title compound, $[\mathrm{Ru^{II}(bpy)_3}]_2$-$[\mathrm{Fe^{III}(CN)_6}]\mathrm{Cl}\cdot 8\mathrm{H_2O}$, (I).

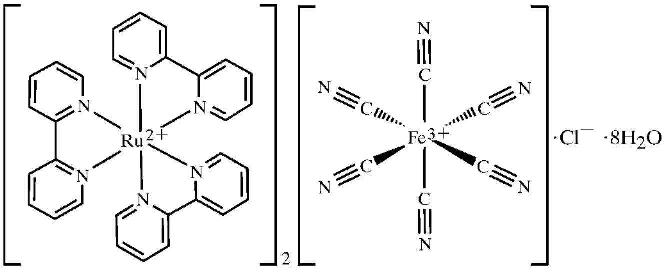

(I)

Several crystal structures of double salts having the same composition type with different metal/halide combinations have been reported, namely $[M_1^{\mathrm{II}}(\mathrm{bpy})_3]_2[M_2^{\mathrm{III}}(\mathrm{CN})_6]X\cdot 8\mathrm{H_2O}$ [$M_1/M_2/X$ = Ru/Co/Cl (refcode HIGZAY; Tamura *et al.*, 1996), Os/Cr/Cl (refcode HIRDOB; Otsuka *et al.*, 1999; corrected as HIRDOB01; Marsh & Spek, 2001), Ru/Cr/Br (HIRDUH01; Otsuka *et al.*, 2001) and Ru/Cr/Cl (HIRFAP01; Otsuka *et al.*, 2001), where 'refcodes' are as assigned by the November 2002 release of the Cambridge Structural Database (Allen, 2002)]. All of these structures were described in space group *C*2. However, it was later pointed out that the structure of HIRDOB should more properly be described in *C*2/*c* (Marsh & Spek, 2001; see also Marsh, 1995). In addition, the structures of HIGZAY, HIRDUH01 and HIRFAP01 may also be described more properly in *C*2/*c*. In this work, we initially decided to describe the structure of (I) in space group *C*2, in which the chloride ion and one of the water O atoms can be located at different sites without disorder, as was done for the analogous systems mentioned above. However, at the suggestion of the co-editor of this paper, the validity of space-group selection has been re-examined. As a result, the final reliability factors in *C*2/*c* and *C*2 have been confirmed to be essentially similar, suggesting that the positional and displacement parameters independently determined for the Cl and O atoms in *C*2 can be considered as artifacts. Thus, space group *C*2/*c* has been judged to be valid in the present case.

The asymmetric unit of (I) consists of an $[\mathrm{Ru^{II}(bpy)_3}]^{2+}$ cation, one-half of an $[\mathrm{Fe^{III}(CN)_6}]^{3-}$ anion, one-half of a chloride anion and four water molecules (Fig. 1). Atom Fe1 is located on an inversion centre. Atoms Cl1 and O1 are assumed to occupy the same site, each having an occupancy of 50%. Atom O2 is located on a twofold axis. Compound (I) possesses an intriguing layered structure (similar to that previously reported for HIGZAY, HIRDOB01, HIRDUH01 and HIRFAP01), in which the layers consisting of the $[\mathrm{Ru^{II}(bpy)_3}]^{2+}$ cations and water molecules, and the layers consisting of the $[\mathrm{Fe^{III}(CN)_6}]^{3-}$ anions and water molecules alternate along the *c* axis (Figs. 2–4). More interestingly, each cationic layer can be understood as a honeycomb layer, in which a water molecule (O2) is encapsulated within each microporous cavity (Fig. 2). An important feature is that the

DOI: 10.1107/S0108270103028841

layer within $0 < z < \frac{1}{2}$, shown in Fig. 2, is made up of the Δ isomers, while the layer within $\frac{1}{2} < z < 1$ only involves the Λ isomers. The structural features of the hexagons are listed in Table 1. Mean-plane calculations reveal that the hexagons containing the Ru1 centres have a planar geometry, where the r.m.s. deviation of the six atoms from the plane of the hexagon is 0.108 Å. When the cavity is viewed along the *c* axis (Fig. 2), it is considered to be elliptical (~3.8 × 2.8 Å in inner diameter, where the van der Waals components of the H atoms are suppressed by assuming a radius of 1.2 Å). The intercationic interactions are stabilized by hydrophobic interactions between the aromatic hydrocarbon moieties, where the shortest C···C distance is ~3.6 Å, and no π–π stacking interactions are observed between the bpy ligands.

The $[\mathrm{Fe^{III}(CN)_6}]^{3-}$ anions and the remainder of the water molecules form two-dimensional sheets based on extensive hydrogen-bonding networks (Figs. 3 and 4, and Table 2). Interestingly, all the components, excluding the axial cyano ligands (C33 and N9), lie in a thin slab of depth 0.0310 (4) Å, one-half of which corresponds to the shift of atom O4 from the plane $z = 0$. Another important feature is that two neighbouring anionic sheets are connected to one another through hydrogen bonds formed between the cyano N atoms (N9) and the water molecules (O2) encapsulated within the micropores [N9···O2 = 2.788 (5) Å]. Thus, interpenetration occurs *via* the formation of a one-dimensional hydrogen-bonding network along the *c* axis (Fig. 5).

The $\mathrm{Fe^{III}}$ ion adopts a nearly regular octahedral geometry, even though the in-plane Fe—C distances [Fe1—C32 = 1.937 (6) Å and Fe1—C31 = 1.942 (6) Å] are slightly shorter than the axial distance [Fe1—C33 = 1.951 (5) Å], where the $\mathrm{Fe(CN)_4}$ plane is assumed to be parallel to the *ab* plane. In addition, the so-called tetragonality ($T = 0.994$) is close to unity. The most remarkable feature is that the hydrogen bonds

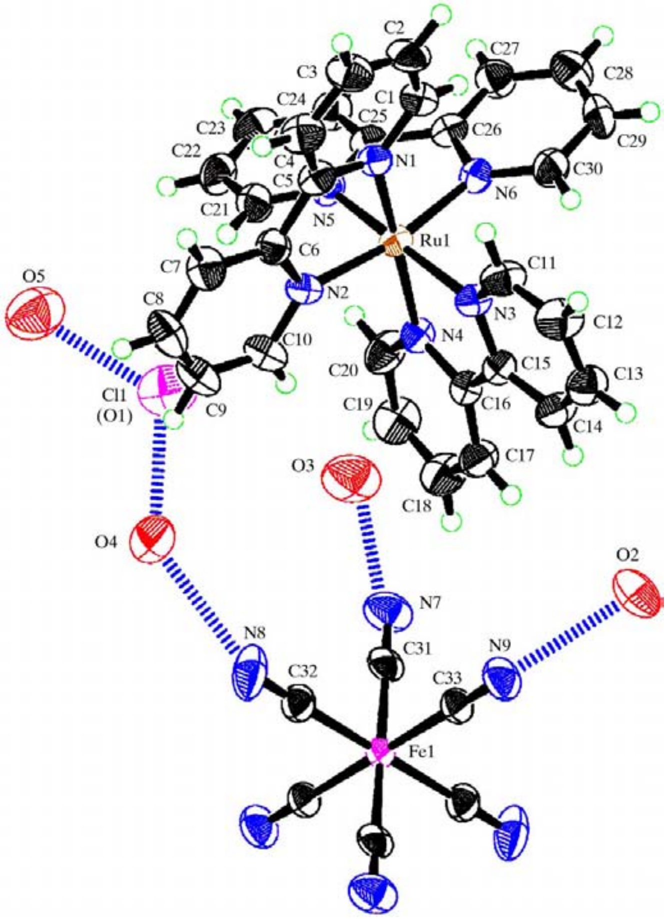

Figure 1
The structure of the asymmetric unit of (I), showing the atom-labelling scheme. Atoms Cl1 and O1 occupy the same site, each with 50% occupancy. Displacement ellipsoids are shown at the 50% probability level and dashed lines denote hydrogen bonds.

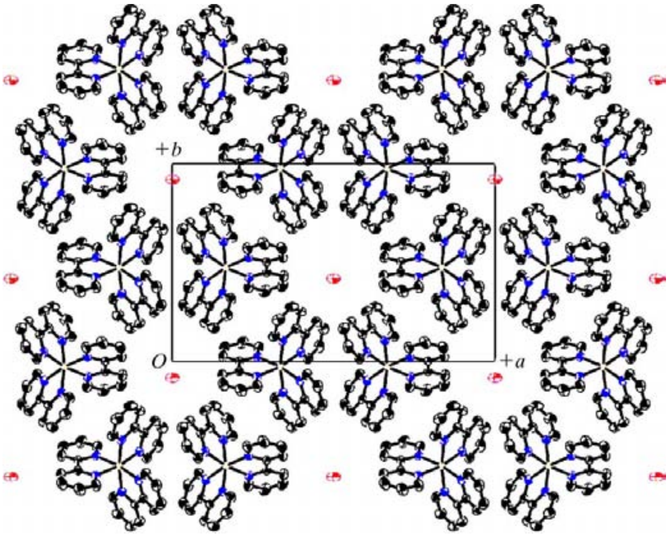

Figure 2
A view along the *c* axis within a layer defined by $0 < z < \frac{1}{2}$, showing a cationic honeycomb sheet consisting of $[\mathrm{Ru^{II}(bpy)_3}]^{2+}$ cations and water molecules (O2). Anionic components and water molecules, shown in Fig. 3, have been omitted for clarity. H atoms have also been omitted for clarity.

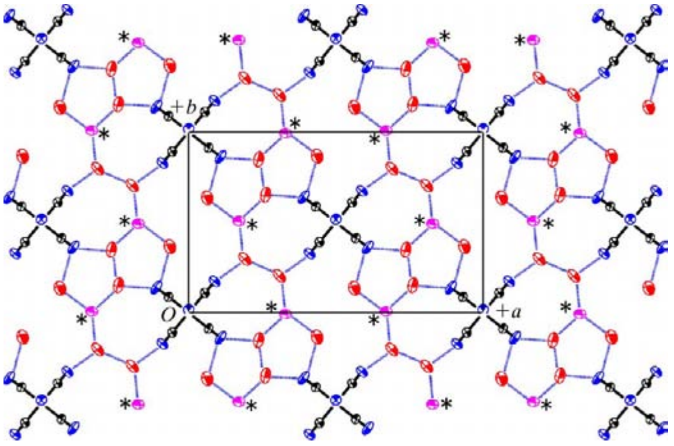

Figure 3
A view along the *c* axis within a layer defined by $-0.15 < z < 0.15$, showing the hydrogen-bonding network consisting of $[\mathrm{Fe^{III}(CN)_6}]^{3-}$ anions and water molecules (O1/O3–O5), leading to the formation of an anionic two-dimensional layer. Dashed lines denote hydrogen bonds. Sites where atoms Cl1 and O1 are disordered are marked with asterisks.

formed between the in-plane cyano ligands and the neighbouring water molecules [N7$\cdots$O3 = 2.855 (7) Å and N8$\cdots$O4 = 2.881 (8) Å] are much weaker than those for the axial cyano ligands, revealing that the in-plane Fe—C bonds possess higher flexibility toward changes in bond lengths that may be induced by the photochemical process discussed below.

It was previously reported that the ^{3}MLCT (MLCT is metal-to-ligand charge transfer) excited state of $[Ru^{II}(bpy)_3]^{2+}$ in (I) is very rapidly quenched, even at 77 K, based on electron-transfer (ET) quenching, affording $[Ru^{III}(bpy)_3]^{3+}$ and $[Fe^{II}(CN)_6]^{4-}$ (Iguro *et al.*, 1994). This outcome was attributed to the fact that the reorganization energy required for the process is small, as a result of the small number of water molecules involved in (I) (Iguro *et al.*, 1994). On the other hand, it was previously reported that the Ru—N distances in $[Ru^{II}(bpy)_3](PF_6)_2$ [2.053 (2) Å, 105 K] are virtually indistinguishable from those in $[Ru^{III}(bpy)_3](PF_6)_3$ [2.057 (3) Å, 105 K; Biner *et al.*, 1992]. Moreover, the Fe^{III}—C(CN) and $Fe^{III}\cdots$N(CN) distances observed in (I) [the Fe^{III}—C(CN) distances are given in Table 1; Fe1$\cdots$N7 = 3.084 (5) Å, Fe1$\cdots$N8 = 3.089 (5) Å and Fe1$\cdots$N9 = 3.094 (5) Å] are similar to those reported for $[Fe^{II}(CN)_6]^{4-}$; for example, Fe^{II}—C(CN) = 1.922 (8)–1.935 (5) Å and $Fe^{II}\cdots$N(CN) = 3.108–3.125 Å for $Li_4[Fe^{II}(CN)_6]\cdot$hexamethylenetetramine$\cdot5H_2O$ (Meyer & Pickardt, 1988). These data show that the change in the molecular volume upon ET quenching is relatively small in both the tris(2,2′-bipyridine)ruthenium and the hexacyanoferrate ions. Consequently, it is considered that a relatively small reorganization energy is required to drive the ET-quenching process, regardless of whether it is undertaken in solution or in the crystal. What can be deduced from the crystal structure of (I) is that the relatively loose hydrogen-bonding character of the in-plane cyano ligands may give rise to the higher flexibility in the in-plane Fe—C bond distances. The present study implies that such structural features may be relevant to the relatively rapid ET-quenching character previously reported for the title double salt (Iguro *et al.*, 1994).

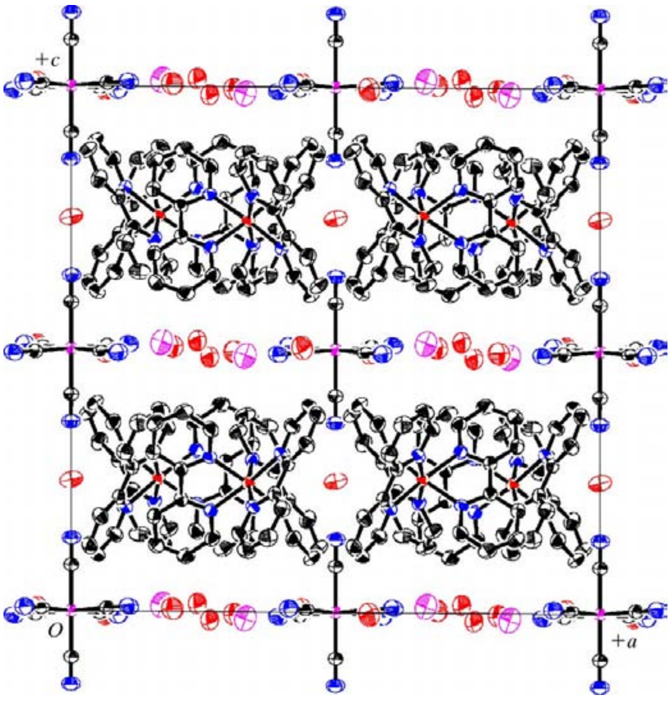

Figure 4
The crystal packing of (I), viewed along the *b* axis. H atoms have been omitted for clarity.

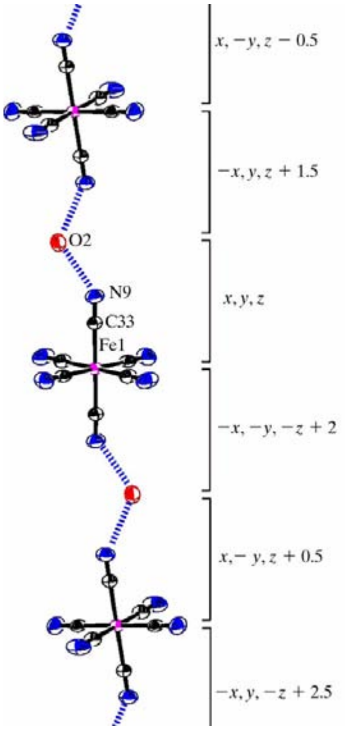

Figure 5
A view of the one-dimensional hydrogen-bonding network formed by the alternate stacking of $[Fe^{III}(CN)_6]^{3-}$ and water molecules, giving rise to interpenetration through the honeycomb layers containing the cations. Dashed lines denote hydrogen bonds.

Experimental

It is often believed that double salts are almost insoluble in water and that their crystals should be grown using so-called diffusion methods. Indeed, a crystalline sample of (I) was previously prepared by a diffusion method (Iguro *et al.*, 1994). Crystals of all the double salts cited in the *Comment* have also been grown by diffusion methods (Tamura *et al.*, 1996; Otsuka *et al.*, 1999, 2001). However, we found that (I) can be recrystallized from hot water in a conventional manner as follows: $[Ru(bpy)_3]Cl_2\cdot6H_2O$ was prepared as previously reported (Fujita & Kobayashi, 1972), except that acetone was used instead of benzene to extract the unreacted bpy. To a solution of $[Ru(bpy)_3]Cl_2\cdot6H_2O$ in a minimum amount of water was added a solution of $K_3[Fe(CN)_6]$ in a minimum amount of water. The brown precipitate was collected by filtration and recrystallized from hot water as follows: an aqueous saturated solution of (I) was prepared at 343 K and filtered while hot. Gradual cooling to room temperature resulted in the growth of good quality red–brown needles of (I). Compound (I) is stable in air at room temperature. Analysis calculated for $C_{66}H_{64}ClFeN_{18}O_8$: C 51.57, H 4.02, N 16.42%; found: C

51.78, H 4.21, N 16.47%. Water content determined by thermogravimetric analysis: 9.42% (calculated); 9.63% (found). The powder X-ray diffractometry of (I) (Cu $K\alpha$) displayed a pattern consistent with that simulated in *TEXSAN* (Molecular Structure Corporation, 2001) based on the crystal structure of (I). The temperature dependence of the magnetic susceptibility of (I) revealed that the effective magnetic moment gradually decreases upon cooling ($\mu_{\rm eff}$ = 2.4 $\mu_{\rm B}$ at 300 K and $\mu_{\rm eff}$ = 1.8 $\mu_{\rm B}$ at 2 K), and this result is indicative of a weak antiferromagnetic character of the material (J values remain undetermined). The X-ray diffraction data were collected using a single crystal that was cut from a well formed needle with a length of a few millimeters.

Crystal data

$[Ru(C_{10}H_8N_2)_3]_2[Fe(CN)_6]Cl\cdot 8H_2O$
M_r = 1530.79
Monoclinic, $C2/c$
a = 22.2498 (17) Å
b = 13.6859 (10) Å
c = 22.1298 (16) Å
β = 90.459 (1)°
V = 6738.5 (9) Å^3
Z = 4
D_x = 1.509 Mg m^{-3}
Mo $K\alpha$ radiation
Cell parameters from 4404 reflections
θ = 2.0–27.1°
μ = 0.76 mm^{-1}
T = 296 (2) K
Needle, red–brown
0.15 × 0.15 × 0.12 mm

Data collection

Bruker SMART APEX CCD area-detector diffractometer
ω scans
Absorption correction: multi-scan (*SADABS*; Sheldrick, 1996)
$T_{\rm min}$ = 0.785, $T_{\rm max}$ = 0.913
20 872 measured reflections
7417 independent reflections
4798 reflections with $I > 2\sigma(I)$
$R_{\rm int}$ = 0.055
$\theta_{\rm max}$ = 27.1°
$h = -28 \rightarrow 28$
$k = -14 \rightarrow 17$
$l = -28 \rightarrow 24$
58 standard reflections
frequency: 330 min
intensity decay: none

Refinement

Refinement on F^2
$R[F^2 > 2\sigma(F^2)]$ = 0.058
$wR(F^2)$ = 0.133
S = 1.15
7417 reflections
435 parameters
H-atom parameters constrained
$w = 1/[\sigma^2(F_o^2) + (0.0284P)^2 + 26.0458P]$ where $P = (F_o^2 + 2F_c^2)/3$
$(\Delta/\sigma)_{\rm max} < 0.001$
$\Delta\rho_{\rm max}$ = 0.53 e Å^{-3}
$\Delta\rho_{\rm min}$ = −0.36 e Å^{-3}

Atoms Cl1 and O1 were assumed to be disordered at the same site, each with 50% occupancy, where the positional and displacement parameters were constrained to be equal. All H atoms, except those of the water molecules, were placed in idealized positions (C—H = 0.93 Å) and included in the refinement as riding, with $U_{\rm iso}$(H) values equal to 1.2$U_{\rm eq}$(C). The water H atoms were not introduced. The highest peak was 0.45 Å from atom O3, while the deepest hole was 0.54 Å from atom Fe1.

Table 1
Selected geometric parameters (Å, °).

Ru1—N6	2.049 (4)	Fe1—C32	1.937 (6)
Ru1—N2	2.051 (4)	Fe1—C31	1.942 (6)
Ru1—N3	2.062 (4)	Fe1—C33	1.951 (5)
Ru1—N4	2.063 (4)	Ru1···Ru1$^{\rm i}$	7.3606 (10)
Ru1—N5	2.071 (4)	Ru1···Ru1$^{\rm ii}$	7.8145 (6)
Ru1—N1	2.072 (4)		
N2—Ru1—N1	78.43 (17)	N3—Ru1—N1	92.97 (16)
N3—Ru1—N4	78.84 (16)	N5—Ru1—N1	95.65 (17)
N6—Ru1—N5	78.90 (17)	C32—Fe1—C33	91.1 (2)
N6—Ru1—N3	95.84 (17)	C32—Fe1—C31	89.2 (2)
N2—Ru1—N3	92.34 (17)	C31—Fe1—C33	89.9 (2)
N6—Ru1—N4	92.49 (17)	C32—Fe1—C31$^{\rm iii}$	90.8 (2)
N2—Ru1—N4	95.31 (17)	C32—Fe1—C33$^{\rm iii}$	88.9 (2)
N2—Ru1—N5	93.88 (17)	C31—Fe1—C33$^{\rm iii}$	90.1 (2)
N4—Ru1—N5	93.08 (16)	Ru1$^{\rm i}$—Ru1—Ru1$^{\rm ii}$	118.757 (6)
N6—Ru1—N1	94.79 (17)	Ru1$^{\rm iv}$—Ru1—Ru1$^{\rm ii}$	122.251 (12)

Symmetry codes: (i) $1-x, y, \frac{3}{2}-z$; (ii) $\frac{1}{2}-x, \frac{1}{2}+y, \frac{3}{2}-z$; (iii) $-x, -y, 2-z$; (iv) $\frac{1}{2}-x, y-\frac{1}{2}, \frac{3}{2}-z$.

Table 2
Selected interatomic distances (Å).

Cl1···O4	2.904 (6)	N7···O3	2.855 (7)
Cl1···O5	2.986 (7)	N8···O4	2.881 (8)
O1···O4	2.904 (6)	O3···O3$^{\rm v}$	2.922 (12)
O1···O5	2.986 (7)	O5···N8$^{\rm vi}$	3.265 (9)
N9···O2	2.788 (5)		

Symmetry codes: (v) $\frac{1}{2}-x, \frac{1}{2}-y, 2-z$; (vi) $\frac{1}{2}-x, -\frac{1}{2}-y, 2-z$.

Data collection: *SMART* (Bruker, 2001); cell refinement: *SAINT* (Bruker, 2001); data reduction: *SAINT*; program(s) used to solve structure: *SHELXS*97 (Sheldrick, 1997); program(s) used to refine structure: *SHELXL*97 (Sheldrick, 1997); molecular graphics: *KENX* (Sakai, 2002); software used to prepare material for publication: *SHELXL*97, *TEXSAN* (Molecular Structure Corporation, 2001), *KENX* and *ORTEP*II (Johnson, 1976).

This work was supported by Grants-in-Aid for Scientific Research on Priority Areas (Nos. 10149248, 11136246 and 12023247, 'metal-assembled complexes') from the Ministry of Education, Science, Sports and Culture of Japan. This work was partly supported by a Grant-in-Aid for Scientific Research (No. 14340223) from the Ministry of Education, Science, Sports and Culture of Japan.

Supplementary data for this paper are available from the IUCr electronic archives (Reference: OB1155). Services for accessing these data are described at the back of the journal.

References

Allen, F. H. (2002). *Acta Cryst.* B**58**, 380–388.

Biner, M., Bürgi, H.-B., Ludi, A. & Röhr, C. (1992). *J. Am. Chem. Soc.* **114**, 5179–5203.

Borgarello, E., Kiwi, J., Pelizzetti, E., Visca, M. & Grätzel, M. (1981). *J. Am. Chem. Soc.* **103**, 6324–6329.

Bruker (2001). *SAINT* (Version 6.22) and *SMART* (Version 5.625). Bruker AXS Inc., Madison, Wisconsin, USA.

Fujita, I. & Kobayashi, H. (1972). *J. Chem. Phys.* **59**, 2902–2908.

Iguro, T., Ikeda, N. & Ohno, T. (1994). *Inorg. Chim. Acta*, **226**, 203–211.

Johnson, C. K. (1976). *ORTEP*II. Report ORNL-5138. Oak Ridge National Laboratory, Tennessee, USA.

Marsh, R. E. (1995). *Acta Cryst.* B**51**, 897–907.

Marsh, R. E. & Spek, A. L. (2001). *Acta Cryst.* B**57**, 800–805.

Meyer, H.-J. & Pickardt, J. (1988). *Acta Cryst.* C**44**, 1715–1717.

Molecular Structure Corporation (2001). *TEXSAN*. Version 1.11r1. MSC, 9009 New Trails Drive, The Woodlands, TX 77381, USA.

Otsuka, T., Sekine, A., Fujigasaki, N., Ohashi, Y. & Kaizu, Y. (2001). *Inorg. Chem.* **40**, 3406–3412.

Otsuka, T., Takahashi, N., Fujigasaki, N., Sekine, A., Ohashi, Y. & Kaizu, Y. (1999). *Inorg. Chem.* **38**, 1340–1347.

Sakai, K. (2002). *KENX*. Graphical User Interface for *SHELXL*97. Tokyo University of Science, Japan.

Sakai, K., Kizaki, Y., Tsubomura, T. & Matsumoto, K. (1993). *J. Mol. Catal.* **79**, 141–152.

Sakai, K. & Matsumoto, K. (1990). *J. Mol. Catal.* **62**, 1–14.

Sheldrick, G. M. (1996). *SADABS*. University of Göttingen, Germany.

Sheldrick, G. M. (1997). *SHELXS*97 and *SHELXL*97. University of Göttingen, Germany.

Tamura, H., Ikeda, N., Iguro, T., Ohno, T. & Matsubayashi, G. (1996). *Acta Cryst.* C**52**, 1394–1399.